EFFECT OF MAIN PIPE VELOCITY ON THE DISCHARGE COEFFICIENT OF A LATERAL OUTLET

Nabil M. Ghali

MAJOR TECHNICAL REPORT

in the

FACULTY OF ENGINEERING

Presented in partial fulfilment of the requirements for

the degree of MASTER OF ENGINEERING

at

Concordia University

Montreal, Canada

August 1975

ABSTRACT

Nabil M. Ghali

EFFECT OF MAIN PIPE VELOCITY ON THE DISCHARGE COEFFICIENT OF A LATERAL ORIFICE

The object of this development project was to design, instal and test an experimental set-up which would permit a study of the flow characteristics of a lateral orifice housed in a pipe. The long-term objective was to evaluate the discharge coefficients of sharp-edged lateral holes set in the wall of a smooth pipe considering the relative hole diameter ratio d/D and the velocity head factor $V^2/2gE$.

The equipment designed was found to operate satisfactorily, a few empirical relations for the lateral orifice discharge coefficients were established using the results of exploratory tests.

ACKNOWLEDGEMENT

The author wishes to express his gratitude to Professor Ramamurthy of the Department of Civil Engineering at Sir George Williams University, Montreal, for suggesting the topic for the development project.

The assistance of Mr. L. Carballada in the initial part of the present project is thankfully acknowledged.

TABLE OF CONTENTS

LIST OF TABLES

LIST OF FIGURES

Chapter 1

INTRODUCTION

The Manifold Problem

In engineering design, a single manifold is often required to supply a fluid to a set of parallel pipes or ducts or to discharge through numerous openings distributed along the length of the manifold. This design concept is adopted in several applications such as fuel burners, sprinkler systems, insecticide spraying, water filtration plants, waste disposal plants, heat exchangers and air coolers.

The commonly encountered design problems are:

(a) determination of the distribution pattern of outlets (size and location) for a predetermined flow pattern along the length of the main pipe;

(b) determination of the discharge and head distribution at the outlet locations for a selected geometric pattern of outlets.

Statement of the Problem

Figure 1 shows schematically the flow through a manifold having a length L, diameter D, hole spacing S, hole diameter d, total inlet flow Q_i, outlet flow Q_o, initial flow velocity V_o and jet velocity V_j.

It was suggested that the factors strongly governing the flow from each individual orifice are the transverse pressure gradient, orifice geometry, conduit geometry and the velocity head factor (see Fig. 2).

(a) Pressure Effect:

It is well known that both inertia and friction effects determine the flow from the manifold. As the fluid flows out through the openings, the velocity head in the main pipe decreases and due to the conservation of energy, the fluid pressure increases. On the other hand, friction effects tend to decrease the pressure along the length of this manifold (Fig. 1). The combined effect of these two factors determines the differential pressure across the outlet which controls the flow through the lateral orifice.

(b) Geometry Effect:

Pipe and orifice geometry, such as shape of pipe, shape of orifice, size of orifice and relative thickness of pipe wall (t/d), number of orifices, spacing, etc. are the geometric parameters that influence the outflow characteristics.

(c) Tangential Velocity Effect:

It was found that the tangential velocity of main flow at the outlet location affects the outflow considerably. Little information is available in this area of fluid mechanics. Furthermore, most papers dealing with the manifold problem have failed to recognize the importance of the velocity head factor $V^2/2gE$.

To study the above effects on the discharge coefficient of a lateral orifice housed in a pipe, a simple test set up was developed as part of the present project. Preliminary tests were conducted and on the basis of these tests, a few tentative conclusions are drawn.

Chapter - 2

REVIEW OF PREVIOUS WORK

Keller (1) reviewed Malishevsky's work and attributes the discrepancy between Malishevsky's expected friction factor and the friction factor obtained by calculations to the variation of the discharge coefficient. Nevertheless, while dealing with the solution of the manifold problem, Keller assumes that the coefficient of discharge C_D of the holes is constant. He also recognized that it is quite possible that the disturbed entrance conditions at the manifold orifices may cause a great variation in the value of C_D for each orifice. Additional tests were recommended to determine the discharge coefficients.

Noseda (2) introduced a method of solving the manifold problem and provided some experimental data on lateral orifice flow. According to him, the mean coefficient of discharge for a certain manifold, as defined by the equation:

$$C_{Dm} = \frac{Q}{\propto\sqrt{2g\propto h_m}\,\Delta S)}$$

varies as a function of the flow.

In the above equation,

Q is the outflow

$\propto$ is the coriolis correction factor

h_m is the mean piezometric head in section S_m

S_m is the length of a section of the manifold

Molz (3) tested a section of a perforated pipe in order to determine the relation between the outflow with both pressure and axial velocity. The results published show that for a given pressure the discharge is a function of the axial velocity. He also concluded that the question concerning outflow from a perforated pipe requires experimental data which provides the relationship Q = Q (P,V).

Bajura (4) presented an analytical investigation of the performance of flow distribution systems for both the intake and the exhaust manifolds, a mathematical model in terms of momentum balance was suggested. Numerical solutions were obtained and compared with experimental data, dimensionless parameters characterizing the performance of manifolds were formulated from the analytical model, the individual effect of discharge coefficients was not evaluated.

Rawn (5) presented a solution for a typical manifold problem using a variable discharge coefficient based on an extension of a theoretical analysis presented by McNown and Hsu.

Vigander (6) determined the value of the coefficient of discharge by modeling the flow inside a corrugated pipe. An open channel flow set-up was used in his studies related to the discharge coefficient of an isolated lateral orifice. The results he obtained were very valuable although one cannot apply these without reservations for sharp-edged orifices set in the pipe walls. It must be noted that his tests were conducted to simulate a field installation in which the corrugations were present in the main pipe.

Michell (7) presented a number of cases of the efflux from the side of a channel. A two-dimensional approach to the flow encountered in manifold was discussed and an equation for C_D was derived.

McNown (8) has adopted the free stream line theory to lateral efflux from a two-dimensional conduit using conformal transformation to obtain solutions of a free efflux and for an efflux with a barrier in the form of a downstream lip. Although the analyses are restricted to two-dimensional irrotational flow, they apply well to pipe manifold systems. Computed curves for different lateral diameter to conduit diameter ratio agree well with measured loss coefficients.

Chapter - 3

EXPERIMENTAL SET-UP AND TESTING PROCEDURE

Discharge Coefficient C_{DE}

The rate of discharge from an orifice or point in the side of a pipe is expressed by:

$$Q = C_{DE}\ a\ \sqrt{2gE}$$

in which C_{DE} is the discharge coefficient, a denotes the cross-sectional area of the port and E is the total head.

For a given diameter ratio d/D the variation of C_{DE} can be expressed as:

$$C_{DE} = C_{DE}\ (R_e,\ V^2/2gE,\ t/d;\ \phi_1,\ \phi_2)$$

where $\frac{VD}{\nu} = R_e$ pipe Reynolds number, $V^2/2gE = \xi$ = velocity factor, t/d = wall thickness factor, ϕ_1 is a variable denoting the shape of the pipe and ϕ_2 is a second order variable denoting the approach flow velocity distribution.

The effect of Reynolds number on the discharge coefficient is considered negligible when the former is very large (turbulent flow). Further, for small t/d values, i.e. for orifices in thin-walled pipes, the control for the orifice flow will be at the sharp-edged entrance, and the flow is less likely to reattach to the orifice wall. Consequently, the parameter t/d does not have a large effect on the value of C_{DE}.

Hence, for a small individual, sharp-edged orifice in a given thin-walled pipe, the rate of discharge can be written:

$$Q = C_{DE}\ (V^2/2gE)\ a\ \sqrt{2gE}$$

The following are the physical dimensions for test pipes selected for the preliminary experimental work conducted to determine C_{DE} $(V^2/2gE)$.

Pipe No.	D_{inch}	d_{inch}	d/D	t_{inch}
1	.512	.297	.580	.0625
2	.750	.250	.333	.0625
3	.500	.125	.250	.0625
4	.750	.125	.166	.0625

Experimental Set-up and Testing Procedure

A centrifugal pump was used to circulate water through plexiglass test pipes. In each of these pipes a hole was drilled and hand-reamed.

To reduce the entrance effect sufficient entry lengths were provided ahead of the orifice. The test pipes were open at both ends and carried pressure taps at 3 inches spacing (Fig. 3).

The pressure taps were connected to a manifold which in turn was linked to a manometer. The test pipe was installed horizontally, the orifice was oriented to have a vertical downward outflow. The experiments were conducted as follows:

The pressure upstream the pipe was adjusted by using an upstream shut-off valve. Three ranges of pressure were selected. Different downstream valve settings provided a range of discharges through the exit pipe which in effect provided a range of velocity head factors.

The pressure profile was taken along the pipe length for each run. The pressure at the orifice location was determined by extrapolating the pressure gradient to the orifice location (Figs. 10, 11, 12 and 13).

The flow out of the orifice was collected in a container for a known time and later weighted to determine the discharge rate.

The flow out of the exit pipe was determined by noting the rise of water level in a large collecting tank (51.5" x 48" x 36") during a known period of time. A stop-watch was used to determine the time intervals. The tests were repeated for different velocity head factors. For this, the pressure gradient across the pipe was changed while supply head pressure was maintained at its initial values.

Chapter - 4

DISCUSSION OF RESULTS

Test Set-up

The test set-up was found to perform satisfactorily and the test pipe sizes were properly selected to suit the pump discharge capacity for providing a wide range of velocity head factors. However, the tests were conducted in less than optimum conditions as far as pressure measurements were concerned. This was partially overcome by providing higher damping in the pressure lines. The various definitions related to the experimental data are shown in Appendix No. 1. A specimen computation is presented in Appendix No. 2.

Discharge Coefficient C_{DE} versus d/D

The experimental results have indicated that, for a given velocity head factor the coefficient of discharge of an orifice is dependent on the diameter ratio d/D. As an example, for velocity head factor $V^2/2gE = 0$, with a value of $d/D = 0.9$, $C_{DE} = 0.67$, while for $d/D = 0.02$, $C_{DE} = 0.605$. This trend can be justified by the effect of pipe curvatures on the wall guidance of the jet flows, as d/D decreases the contraction in the plan perpendicular to the pipe axis increases. It should be noted that as d/D decreases to approach zero, the situation approaches the case of flow passing a flat plate and C_{DE} decreases to reach the value 0.61 (Fig. 9).

Discharge Coefficient C_{DE} versus $V^2/2gE$

The results show also that the discharge coefficient for a given diameter ratio d/D is dependent on the velocity head factor $V^2/2gE$ (see

Tables 1, 2, 3 and 4). As an example, for $d/D = 0.58$, the value of C_{DE} is 0.67 at $V^2/2gE = 0$, while at $V^2/2gE = 0.7$, C_{DE} decreases to 0.24.

The relation obtained for the variation of C_{DE} is a straight line equation. The constants of the fitting line are dependent on d/D. The above can be justified by increasing the main velocity inside the pipe which increases the jet angle and reduces the cross-sectional area normal to the velocity factor (Fig. 8).

Variation of C_{DE} with t/d

An attempt to evaluate the effect of the wall thickness at the orifice locations was carried out. Half the wall thickness of pipe No. 2 at the orifice location was removed and a set of experimental tests was carried out. The points obtained were within the scatter of the results with no general trend.

Variation of C_{DE} with P

The effect of pressure in the main pipe on C_{DE} for orifice outflow was not noticeable, as one might expect. The values of C_{DE} obtained for different ranges of pressure did not display any trends.

Jet Angle

The jet inclination to the pipe axis increased as the main pipe velocity increased. No detailed jet angle measurements were made since the jet sometimes came out as spray (Fig. 3).

Chapter - 5

CONCLUSIONS AND SCOPE FOR FURTHER WORK

Conclusions

The equipment developed to study the discharge coefficients of lateral pipe orifices was found to perform satisfactorily.

The following conclusions are presented on the test results and interpretation of earlier available data:

The coefficient of discharge of a lateral orifice C_{DE} is a function of the diameter ratio d/D, the higher the diameter ratio the higher the value of C_{DE}. The coefficient of discharge of a sharp-edged orifice in the side of a thin-walled pipe is also dependent on the main pipe velocity factor $V^2/2gE$, the governing equation can be approximated by a straight line of the following form:

$$C_{DE} = A - B(V^2/2gE)$$

where A and B are constants for a given d/D ratio.

The variation of the coefficient of discharge with the velocity factor does not depend on the absolute value of pressure drop across the orifice for the range of reference pressures tested. The effect of wall thickness t/d on the coefficient of discharge C_{DE} was found to be very small and within the scatter of results. The jet angle of the outflow through the orifice increases with the increase of velocity factor. Although it was concluded that the effect of wall thickness is small in the range of t/d tested, it is conceivable that t/d will have a considerable effect as t/d is increased to a very large value. A degenerate case of this is the combination of a pipe attachment to the lateral orifice.

Scope for further work

It is expected that round-edged orifices will have a higher coefficient of discharge compared with the sharp-edged orifice. A series of tests where a round-edged orifice is used are recommended.

The results obtained for single outlets can be used toward obtaining a meaningful solution for the thermal diffusion problems since the area distribution for a given flow can be adjusted, in a multiport system. The effect of Reynolds number based on outlet geometry (fig. 14 & 15) can also be studied to improve the predicted outflow characteristics.

APPENDIX No. 1

NOMENCLATURE

D	Internal pipe diameter inch
d	Hole diameter inch
a	Hole cross sectional area sq. inch
H	Piezometric head at hole location inch of mercury above atmospheric pressure
$\overline{X}$	Discharge through the hole lb/sec.
$\overline{Y}$	Rate of increase in height in the water collecting tank cm/sec.
Q_{th}	Theoretical hole discharge cu.in/sec.
Q_A	Actual hole discharge cu. in/sec.
Q_O	Main pipe out flow discharge
C_{DH}	Discharge coefficient defined by the equation $C_{DH} = \frac{Q_A}{9\sqrt{2gH}}$
C_{DE}	Discharge coefficient defined by the equation $C_{DE} = \frac{Q_A}{9\sqrt{2gE}}$
V	Main pipe velocity downstream of hole ft/sec.
ξ	Velocity head factor $= \frac{V^2}{2gE}$
t	Pipe wall thickness inch
P	Pressure reading inch mercury
P_o	Zero pressure reading inch mercury

APPENDIX No. 2

Specimen Computation:

Run No.: 807-3A-2 (Fig. 11 b.)

1. Pipe data:

Hole diameter d = .25"

Pipe diameter D = .75"

$d/D = \frac{.25}{.75} = .33$

2. Collecting Tank Dimensions:

51.5" x 48" LG

Tank surface area $= \frac{51.5 \times 48}{144} = 17.166$ sq. ft.

3. Container Initial Weight = 2.25 lb

Pressure tap no. at hole location = 11

4. Observed Data

Discharge through the hole Q_A

19.75 - 2.25 = 17.5 lb in 43 sec.

Flow out of the pipe Q_O

10 cm rise in tank in 65 sec.

Pressure Gradient (inch of mercury)

Hole location	P	Hole location	P	Hole location	P
1	35.90	6	28.60	11	23.30
2	34.75	7	27.10	12	21.30
3	32.60	8	26.10	13	20.40
4	30.70	9	25.20	14	21.20
5	30.65	10	24.70	15	20.00

Datum Reading $P_o = 1.65$

Corrected Pressure Value at Orifice Location - see Fig. 11

$20'' - 1.65'' = 18.35''$

$Q_A = \frac{17.5 \times 1728}{62.4 \times 43} = 10.8$ cu.in./sec.

$Q_{TH} = A\sqrt{2gH} = \frac{\pi}{4} d^2 \sqrt{2 \times 32.2 \times 13.6 \times 12 \times h}$

$= \frac{\pi}{4} (.25)^2 \sqrt{2 \times 32.2 \times 13.6 \times 12 \times 18.35}$

$= 0.04906 \times \sqrt{192800}$

$= 0.04906 \times 439$

$= 21.5$ cu.in./sec

$C_{DH} = \frac{Q_A}{Q_{TH}} = \frac{10.8}{21.5} = .502$

Outlet Velocity ft/sec.

$V = \frac{4Q_0}{\pi D^2} = \frac{4 \times 17.166 \times 10 \times 12}{\pi \times 2.54 \times 65 \times .75^2} = 28.61$

$V^2 = 821$ ft^2/sec^2

$\alpha = \frac{V^2}{2gH} = \frac{821 \times 144}{2 \times 32.2 \times 13.6 \times 12 \times 18.35} = .631$

$\varphi = \frac{\alpha}{\alpha + 1} = \frac{.613}{1.613} = .380$

$C_{DE} = C_{DH} \sqrt{1 - \varphi} = .613 \sqrt{1 - .380}$

$= .613 \sqrt{.62} = .395$

BIBLIOGRAPHY

1. Keller, J.D. "The Manifold Problem" J. Appl. Mech. 16, March 1949, pp. 77-85
2. Noseda, G. "Experimental Study on Pipes with Rate of Flow Decreasing along their length" IAHR General Meeting Trans., Vol. II, Lisbon 1957, pp. D 8-1-9
3. Molz, F.J. "Effect of Axial Flow on Perforated Pipe Outflow", J. of Hydr. Div. Proc. ASCE H 74, April 1972, pp. 747-750
4. Bajura, R.A. "A Model for Flow Distribution in Manifolds", Journal of Engineering for Power, January 1971, Trans. of the ASME
5. Rawn, A.M. "Diffusers for Disposal of Sewage in Sea Water", Trans. ASCE, Vol. 126, Part III, 1961, pp. 344-388
6. Vigander, S., Elder, R.A. and Brooks, N.H. "Internal Hydraulics of Thermal Discharge Diffusers", J. of Hydr. Div., Proc. ASCE, HY. 2, February 1970, pp. 509-527
7. Michell, J.H. "On the Theory of Free Stream Lines" Philosophical Transactions of Royal Society of London, Vol. A181, 1890, pp. 389-431
8. McNown, J.S. and Hsu, E.Y. "Application of Conformal Mapping to Divided Flow", Proc. Midwestern Conf. on Fluid Dynamics, 1st Conf. 1950, pp. 143-155
9. National Advisory Committee for Aeronautics "Technical Memorandum 952", Washington D.C., September 1940

Table 1
REDUCED DATA FOR PIPE* NO 1

PIPE NO 1
D = .512", d = .297"
d/D = .58 (see Fig. 4)

RUN NO	Q_A	Q_{TH}	C_{DH}	$V^2/2gH$	C_{DE}	$V^2/2gE$
722.2A-1	26.66	39.35	.678	0	.678	0
722.2B-1	20.74	31.56	.656	0	.656	0
722.2C-1	14.90	22.30	.668	0	.668	0
805.2A-1	23.58	35.89	.657	0	.657	0
907.2A-1	23.54	35.79	.657	0	.657	0
907.2A-2	19.80	30.58	.647	.064	.627	.060
805.2A-2	19.99	30.14	.663	.099	.632	.090
722.2A-3	19.05	32.17	.591	.145	.553	.126
722.2B-3	14.31	25.32	.564	.173	.520	.147
722.2C-2	9.67	16.76	.574	.198	.523	.165
907.2A-3	15.78	26.57	.594	.230	.536	.187
805.2A-3	16.42	26.64	.616	.254	.550	.200
805.2A-4	14.10	24.38	.577	.397	.489	.284
907.2A-4	10.80	21.07	.515	.756	.390	.430
805.2A-5	9.41	18.78	.501	1.060	.347	.514
907.2A-5	8.58	17.54	.498	1.272	.324	.560
722.2C-5	4.34	9.13	.475	1.790	.285	.640
907.2A-6	7.01	15.58	.448	1.943	.262	.660
907.2A-7	5.74	13.23	.432	2.803	.221	.737
907.2A-8	4.89	11.96	.408	3.500	.192	.777
722.2B-5	3.36	10.17	.329	4.040	.147	.801
722.2A-5	3.10	10.39	.298	6.580	.108	.868
907.2A-9	2.99	8.40	.356	8.200	.117	.891
805.2A-6	2.58	6.72	.383	13.720	.100	.932

* FOR OBSERVED DATA SEE TABLE NO. 6

Table 2

REDUCED DATA FOR PIPE* No 2

PIPE NO 2
D = .75", d = .25
d/D = .33 (see Fig. 5)

RUN No	Q_A	Q_{TH}	C_{DH}	$V^2/2gH$	C_{DE}	$V^2/2gE$
723.3A-1	17.94	29.15	.615	0	.615	0
723.3B-1	14.23	22.78	.625	0	.625	0
723.3C-1	10.72	17.15	.625	0	.625	0
807.3A-1	18.13	27.76	.653	0	.653	0
723.3B-2	11.52	19.50	.591	.210	.537	.173
723.3C-2	8.08	14.16	.571	.253	.513	.200
723.3B-3	9.04	17.15	.527	.469	.435	.319
723.3C-3	7.15	13.13	.545	.476	.450	.322
807.3A-2	10.80	21.51	.502	.613	.395	.380
723.3A-2	10.28	20.33	.506	.778	.380	.437
723.3A-3	7.67	18.52	.414	1.137	.283	.532
807.3A-3	6.92	17.24	.400	1.277	.265	.560
723.3C-4	3.92	10.04	.390	1.320	.256	.568
723.3B-4	4.32	10.97	.393	2.323	.248	.699
723.3A-4	4.43	12.94	.342	3.110	.168	.756
807.3A-4	4.38	12.64	.346	3.450	.164	.776
807.3A-5	1.57	5.83	.270	20.550	.064	.953

* FOR OBSERVED DATA SEE TABLE No 7

TABLE 3

REDUCED DATA FOR PIPE* No 3

PIPE NO 3
D = .5", d = .125"
d/D = .25 (see Fig. 6)

RUN No	Q_A	Q_{TH}	C_{DH}	$V^2/2gH$	C_{DE}	$V^2/2gE$
803.2A-1	4.06	6.51	.623	0	.623	0
803.2A-2	3.24	5.53	.587	.114	.550	.102
803.2A-3	2.57	4.98	.516	.326	.450	.246
803.2A-4	1.97	3.96	.497	.783	.365	.440
803.2A-5	1.32	3.15	.419	1.754	.252	.637
803.2A-6	.35	1.50	.231	9.810	.070	.910

* FOR OBSERVED DATA SEE TABLE No 8

TABLE 4

REDUCED DATA FOR PIPE* No 4

PIPE NO 4
D = .75", d = .125"
d/D = .166 (see Fig. 7)

RUN No	Q_A	Q_{TH}	C_{DH}	$V^2/2gH$	C_{DE}	$V^2/2gE$
1012.3A-1	4.54	7.33	.620	0	.620	0
1012.3A-2	3.40	6.07	.559	.202	.509	.168
1012.3A-3	2.91	5.49	.530	.398	.448	.284
1012.3A-4	2.51	5.15	.488	.620	.383	.383
1012.3A-5	2.33	4.72	.488	.940	.350	.484
1012.3A-6	1.97	4.42	.446	1.350	.292	.575
1012.3A-7	1.48	3.49	.427	2.350	.233	.701
1012.3A-8	1.11	2.95	.378	3.429	.179	.774

* FOR OBSERVED DATA SEE TABLE No 9

Table 5

TEST RESULTS FOR DEAD END PIPES

(see Fig. 9)

D	d	d/D	C_{DE}
2.750	2.000	.727	.673
.512	.297	.580	.660
2.750	1.000	.363	.625
.750	.250	.330	.625
.500	.125	.250	.623
.750	.125	.166	.620
2.750	.375	.136	.607

TABLE 6 RAW DATA FOR PIPE NO. 1

D = .512" d = .297" d/D = .58

RUN NO.	$\bar{X}$	Q_A	H	$\frac{2gH}{100}$	$\sqrt{2gH}$	Q_{TH}	C_{DH}	$\bar{Y}$	V	V^2	$\frac{V^2}{2gH}$	C_{DE}	$\frac{V^2}{2gE}$
722.2A-1	.963	26.66	30.85	3242	568	39.35	.678	0	0	0	0	.678	0
722.2A-3	.688	19.05	20.65	2170	465	32.17	.591	.037	14.83	2199	.145	.553	.126
722.2A-5	.112	3.10	2.15	225	150	10.39	.298	.082	32.12	1031	6.580	.108	.868
722.2B-1	.749	20.74	19.75	2075	456	31.56	.656	0	0	0	0	.656	0
722.2B-3	.517	14.31	12.75	1340	366	25.32	.564	.032	12.67	1605	.173	.520	.147
722.2B-5	.121	3.36	2.05	215	147	10.17	.329	.062	24.57	6037	4.040	.147	.801
722.2C-1	.538	14.9	9.85	1035	322	22.30	.668	0	0	0	0	.668	0
722.2C-3	.347	9.62	5.60	588	242	16.76	.574	.022	9.01	81.2	.198	.523	.165
722.2C-5	.157	4.34	1.65	173	132	9.13	.475	.037	14.68	215.5	1.790	.285	.640
805.2A-1	.851	23.58	25.70	2701	519	35.89	.657	0	0	0	0	.657	0
805.2A-2	.722	19.99	18.00	1891	435	30.14	.663	.029	11.43	130.6	.099	.632	.090
805.2A-3	.593	16.42	14.10	1481	385	26.64	.616	.041	16.17	261.5	.254	.550	.200

TABLE 6 (cont'd) RAW DATA FOR PIPE NO. 1

D = .512" d = .297" d/D = .58

RUN NO.	$\bar{X}$	Q_A	H	$\frac{2gH}{100}$	$\sqrt{2gH}$	Q_{TH}	C_{DH}	$\bar{Y}$	V	V^2	$\frac{V^2}{2gH}$	C_{DE}	$\frac{V^2}{2gE}$
805.2A-4	.509	14.10	11.80	1240	352	24.38	.577	.047	18.50	342.2	.397	.489	.284
805.2A-5	.340	9.41	7.00	735	271	18.78	.501	.059	23.26	541.0	1.060	.347	.514
805.2A-6	.093	2.58	.90	94	97	6.72	.383	.076	30.00	900.0	13.72	.100	.932
907.2A-1	.850	23.54	25.45	2674	517	35.79	.657	0	0	0	0	.657	0
907.2A-2	.714	19.80	18.75	1970	444	30.58	.647	.023	9.36	87.6	.064	.627	.060
907.2A-3	.570	15.78	14.00	1471	384	26.57	.594	.039	15.34	235.3	.232	.536	.187
907.2A-4	.390	10.80	8.85	930	304	21.07	.515	.056	22.00	484.0	.756	.390	.430
907.2A-5	.310	8.58	6.10	641	253	17.54	.489	.060	23.80	566.4	1.272	.324	.560
907.2A-6	.250	7.01	4.85	509	225	15.58	.448	.066	26.20	686.9	1.943	.26[illegible]	.660
907.2A-7	.207	5.74	3.50	367	191	13.23	.432	.068	26.73	714.5	2.803	.221	.737
907.2A-8	.175	4.89	2.85	299	173	11.96	.408	.068	26.96	726.4	3.500	.192	.777
907.2A-9	.108	2.99	1.40	147	121	8.40	.356	.073	28.93	836.9	8.200	.117	.891

TABLE 7 RAW DATA FOR PIPE NO.2

D = .75"   d = .25"   d/D = .33

RUN NO.	$\bar{X}$	Q_A	H	$\frac{2gH}{100}$	$\sqrt{2gH}$	Q_{TH}	C_{DH}	$\bar{Y}$	V	V^2	$\frac{V^2}{2gH}$	C_{DE}	$\frac{V^2}{2gE}$
723.3A-1	.648	17.94	33.65	3536	595	29.15	.615	0	0	0	0	.615	0
723.3A-2	.371	10.28	16.35	1719	415	20.33	.506	.166	30.4	929	.778	.380	.437
723.3A-3	.277	7.67	13.65	1428	378	18.52	.414	.183	33.6	1128	1.137	.283	.532
723.3A-4	.160	4.43	6.85	719	268	12.94	.342	.215	39.4	1559	3.110	.168	.756
723.3B-1	.514	14.23	20.65	2170	465	22.78	.625	0	0	0	0	.625	0
723.3B-2	.416	11.52	15.10	1587	398	19.50	.591	.083	15.2	232	.210	.537	.173
723.3B-3	.326	9.04	11.65	1227	350	17.15	.527	.109	20.0	400	.469	.435	.319
723.3B-4	.156	4.32	4.75	502	224	10.97	.393	.155	28.4	810	2.323	.248	.699

TABLE 7 (cont'd) RAW DATA FOR PIPE NO. 2

D = .75" d = .25" d/D = .33

RUN NO.	$\bar{X}$	Q_A	H	$\frac{2gH}{100}$	$\sqrt{2gH}$	Q_{TH}	C_{DH}	$\bar{Y}$	V	V^2	$\frac{V^2}{2gH}$	C_{DE}	$\frac{V^2}{2gE}$
723.3C-1	.387	10.72	11.70	1229	350	17.15	.625	0	0	0	0	.625	0
723.3C-2	.292	8.08	7.95	835	289	14.16	.571	.066	12.2	147	.253	.510	.200
723.3C-3	.258	7.15	6.85	719	268	13.13	.545	.084	15.4	238	.476	.450	.322
723.3C-4	.141	3.92	4.00	420	205	10.04	.390	.107	19.6	386	1.320	.256	.568
807.3A-1	.655	18.13	30.55	3210	566	27.76	.653	0	0	0	0	.653	0
807.3A-2	.390	10.80	18.35	1928	439	21.51	.502	.156	28.6	821	.613	.395	.380
807.3A-3	.250	6.92	11.85	1245	352	17.24	.400	.181	33.2	1105	1.277	.265	.560
807.3A-4	.158	4.38	6.35	667	258	12.64	.346	.218	40.0	1603	3.450	.164	.776
807.3A-5	.057	1.57	1.35	141	119	5.83	.270	.245	44.9	2025	20.55	.064	.953

TABLE 8 RAW DATA FOR PIPE NO.3

D = .5"   d = .125"   d/D = .25

RUN NO.	$\bar{X}$	Q_A	H	$\frac{2gH}{100}$	$\sqrt{2gH}$	Q_{TH}	C_{DH}	$\bar{Y}$	V	V^2	$\frac{V^2}{2gH}$	C_{DE}	$\frac{V^2}{2gE}$
803.2A-1	.146	4.06	27.15	2853	534	6.51	.623	0	0	0	0	.623	0
803.2A-2	.117	3.24	19.60	2059	453	5.53	.587	.031	12.8	164	.114	.550	.102
803.2A-3	.092	2.57	15.85	1665	408	4.98	.516	.047	19.4	377	.326	.450	.246
803.2A-4	.071	1.97	10.05	1056	325	3.96	.497	.058	23.9	574	.783	.365	.440
803.2A-5	.047	1.32	6.35	667	258	3.15	.419	.069	28.5	813	1.754	.252	.637
803.2A-6	.012	.35	1.45	152	123	1.50	.231	.078	32.2	1039	9.810	.070	.910

TABLE 9 RAW DATA FOR PIPE NO. 4

$D = .75''$ $d = .125''$ $d/D = .166$

RUN NO.	$\bar{X}$	Q_A	H	$\frac{2gH}{100}$	$\sqrt{2gH}$	Q_{TH}	C_{DH}	$\bar{Y}$	V	V^2	$\frac{V^2}{2gH}$	C_{DE}	$\frac{V^2}{2gE}$
1012.3A-1	.164	4.541	33.85	3557	597	7.33	.620	0	0		0	.620	0
1012.3A-2	.123	3.400	23.35	2454	495	6.07	.559	.101	18.5	344	.202	.509	.168
1012.3A-3	.105	2.908	19.00	1996	447	5.49	.530	.128	23.5	552	.398	.448	.284
1012.3A-4	.091	2.517	17.00	1786	422	5.15	.488	.151	27.7	769	.620	.383	.383
1012.3A-5	.084	2.337	14.50	1523	390	4.72	.488	.172	31.6	998	.940	.350	.484
1012.3A-6	.071	1.974	12.35	1297	360	4.42	.446	.190	34.9	1217	1.350	.292	.575
1012.3A-7	.054	1.488	7.70	809	284	3.49	.427	.198	36.4	1322	2.350	.233	.701
1012.3A-8	.040	1.115	5.50	578	240	2.95	.378	.202	37.1	1376	3.429	.179	.774

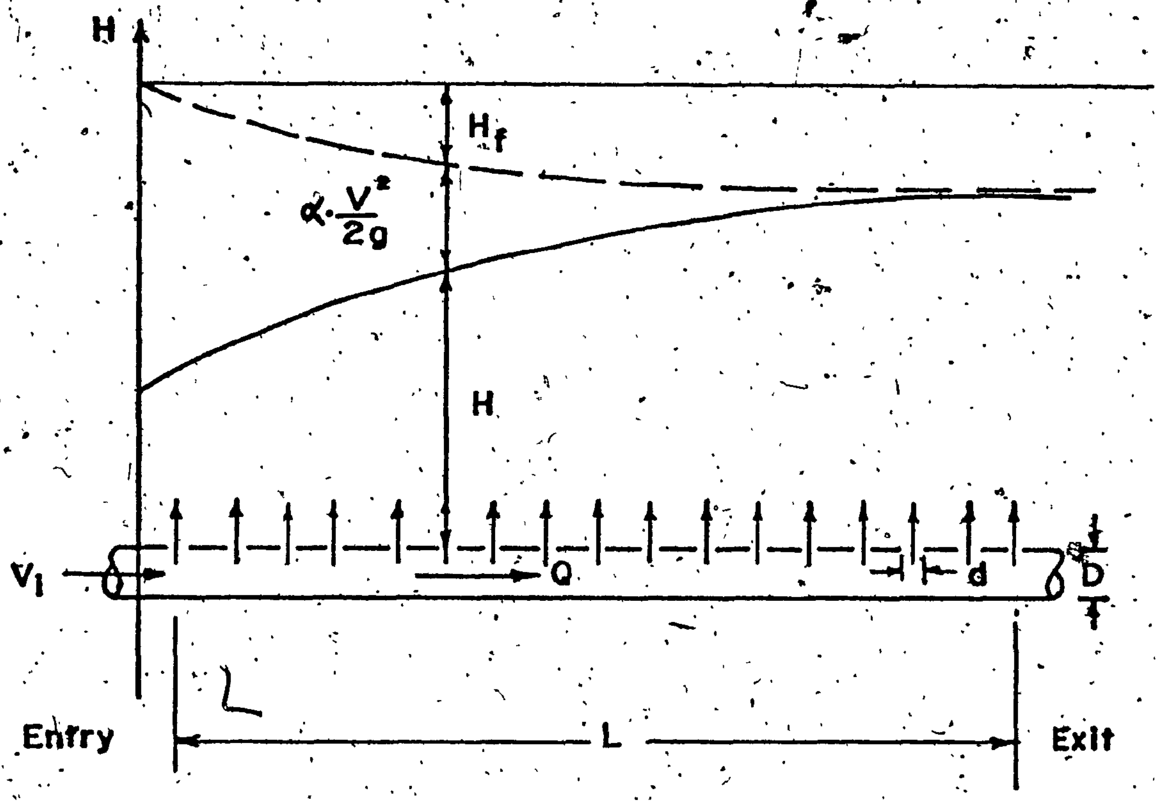

FIG. 1 FLOW THROUGH MANIFOLD

$$\frac{P - Pa}{\alpha} = \Delta H$$

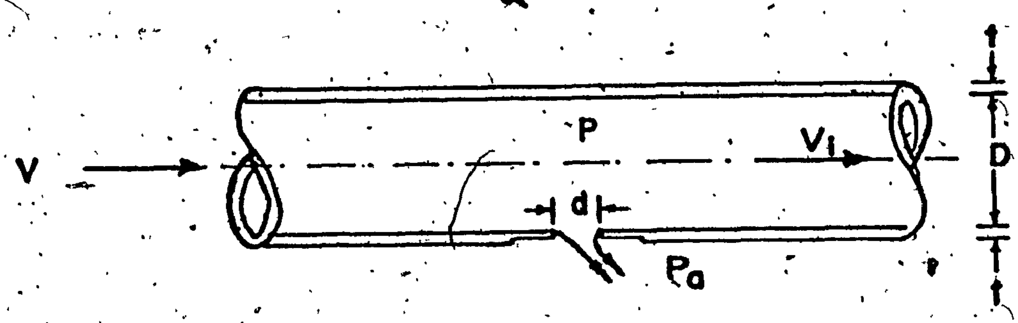

FIG. 2 DEFINITION SKETCH

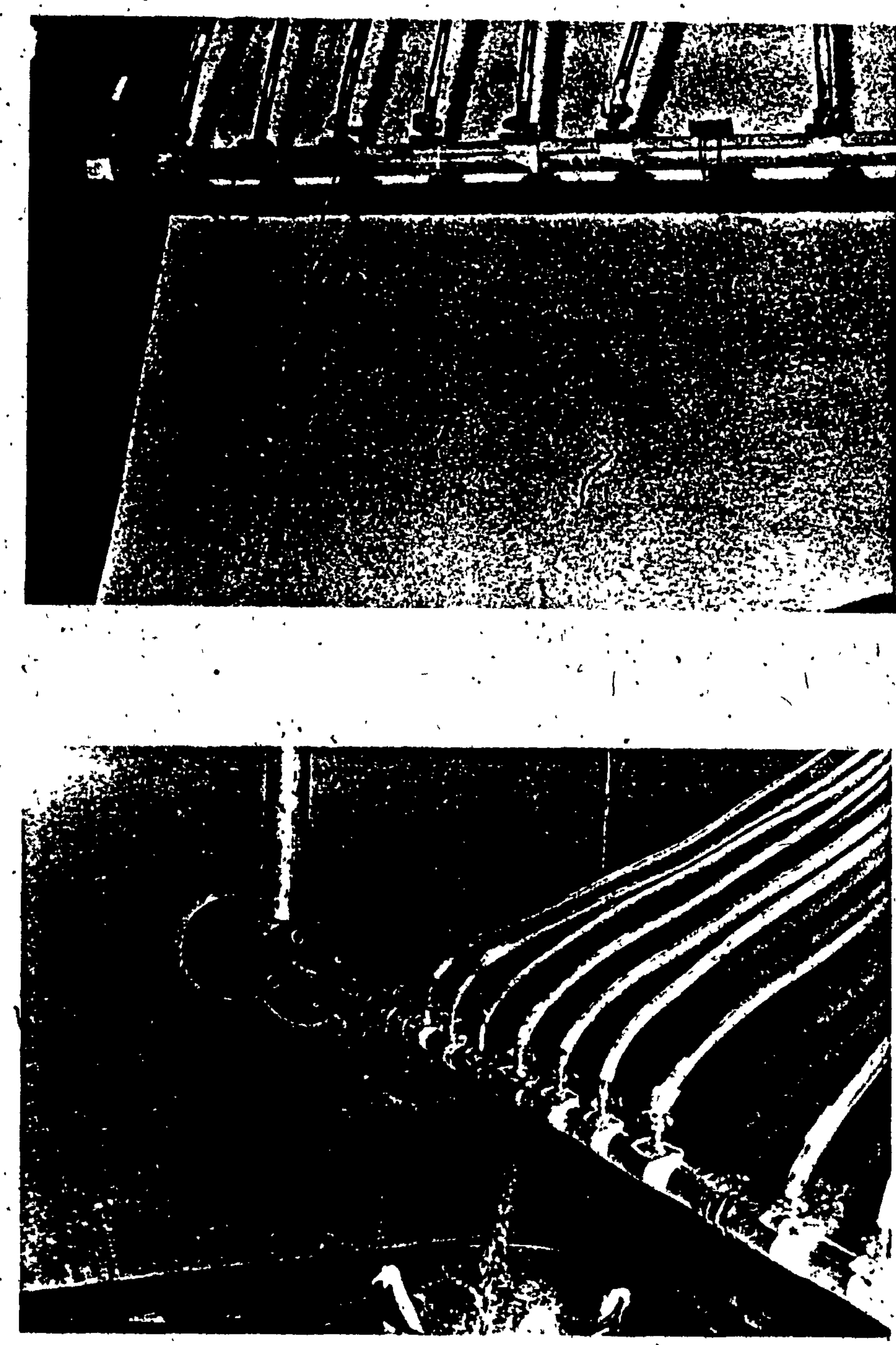

Fig. 3 - PIPE UNDER TEST

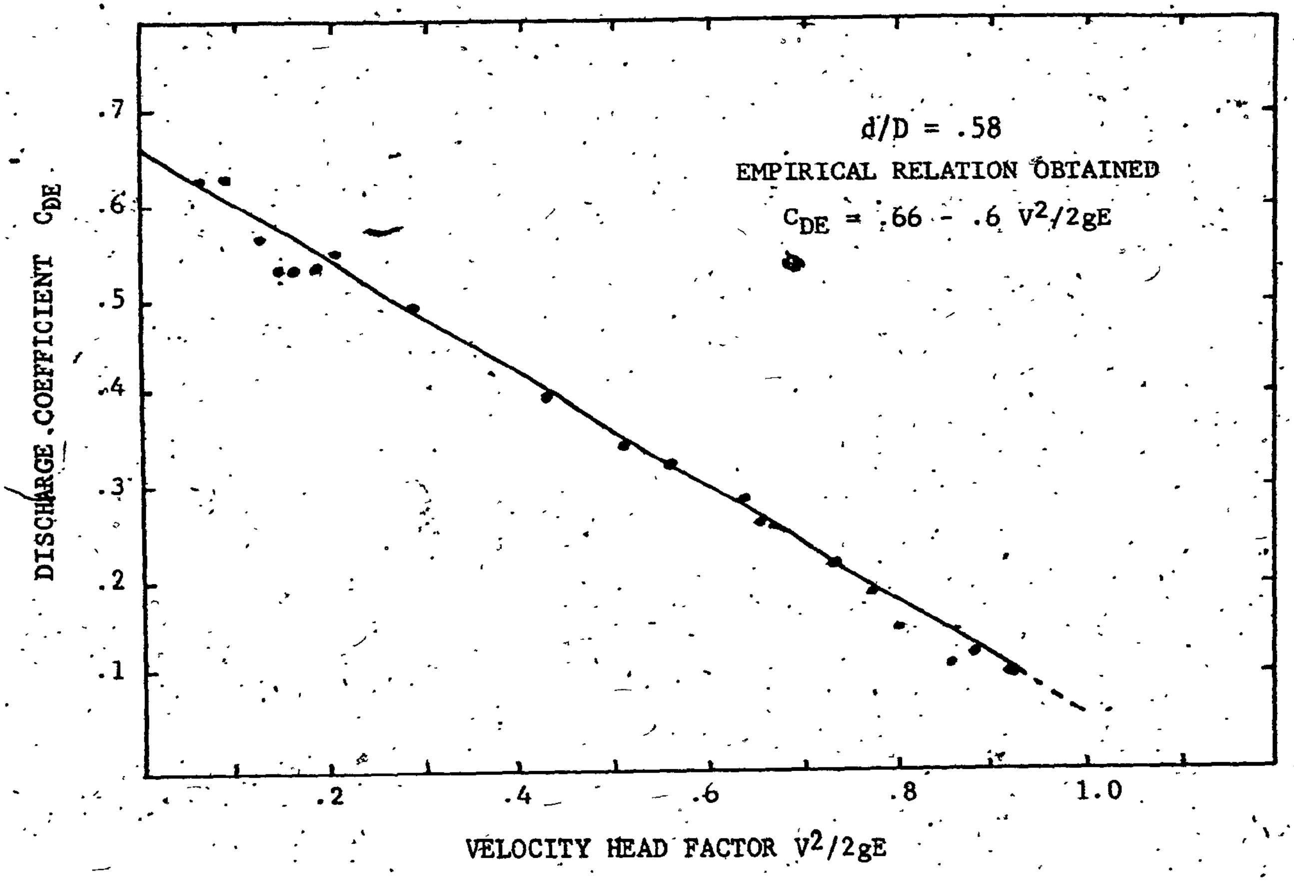

Fig. 4. - DISCHARGE COEFFICIENT FOR PIPE No. 1

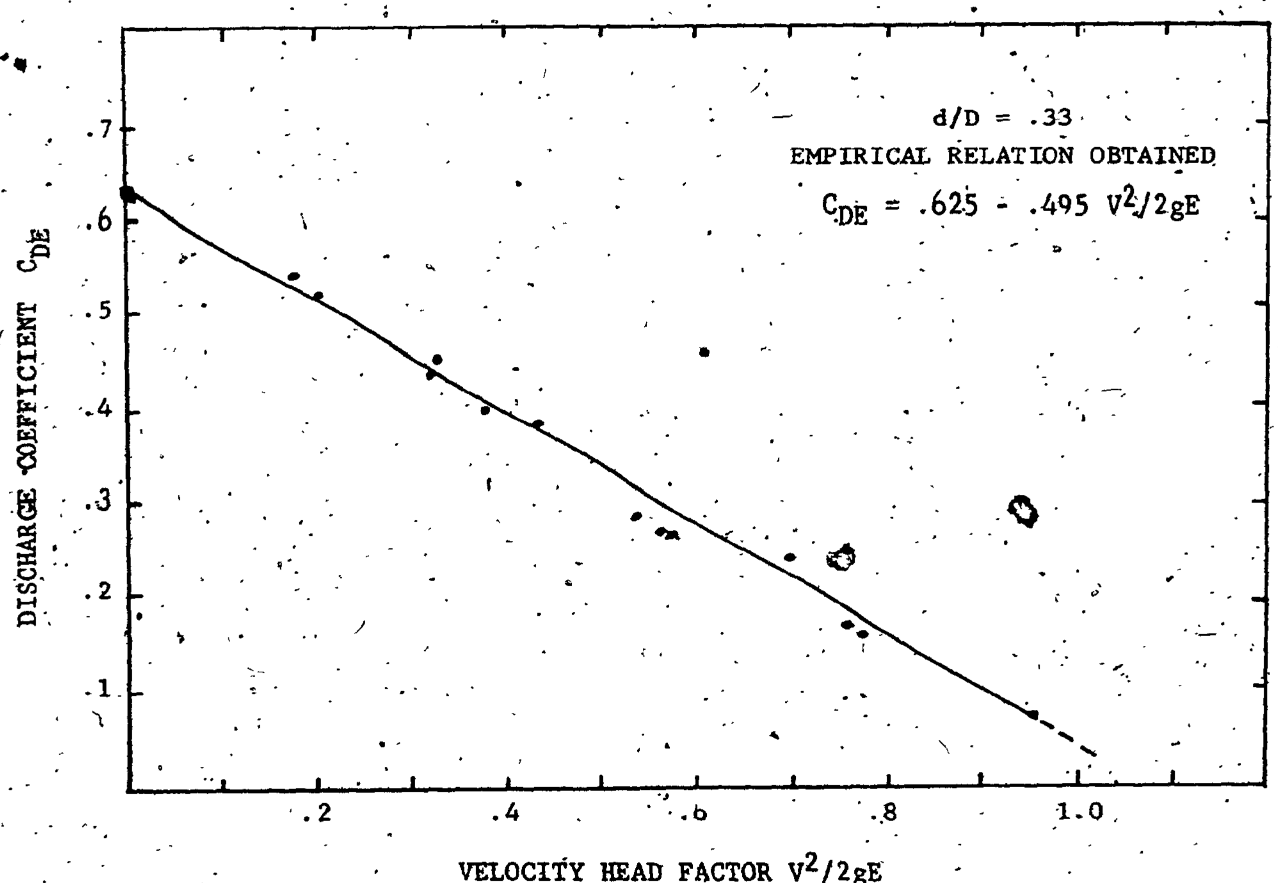

Fig. 5 - DISCHARGE COEFFICIENT FOR PIPE No. 2

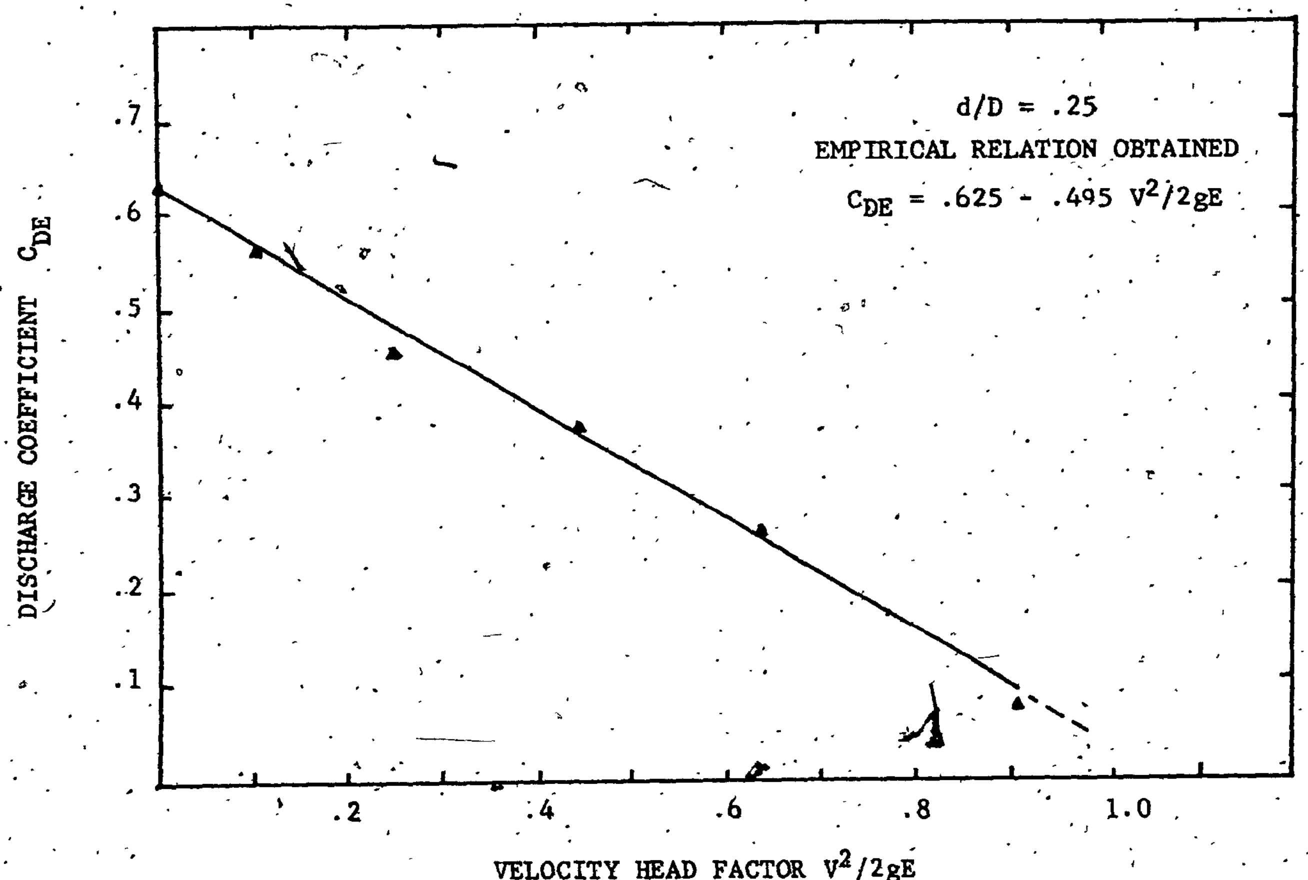

Fig. 6 - DISCHARGE COEFFICIENT FOR PIPE No. 3

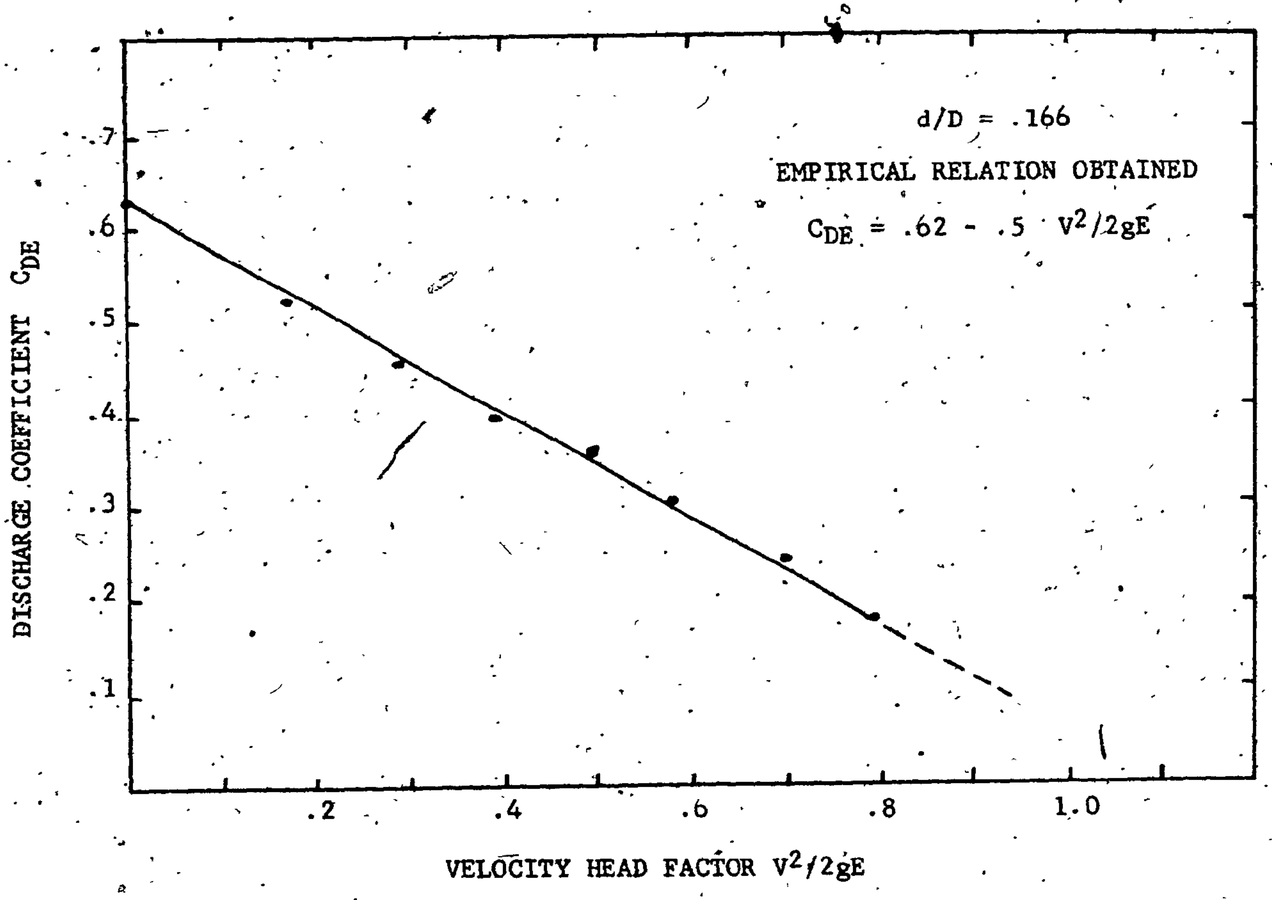

Fig. 7 - DISCHARGE COEFFICIENT FOR PIPE No. 4

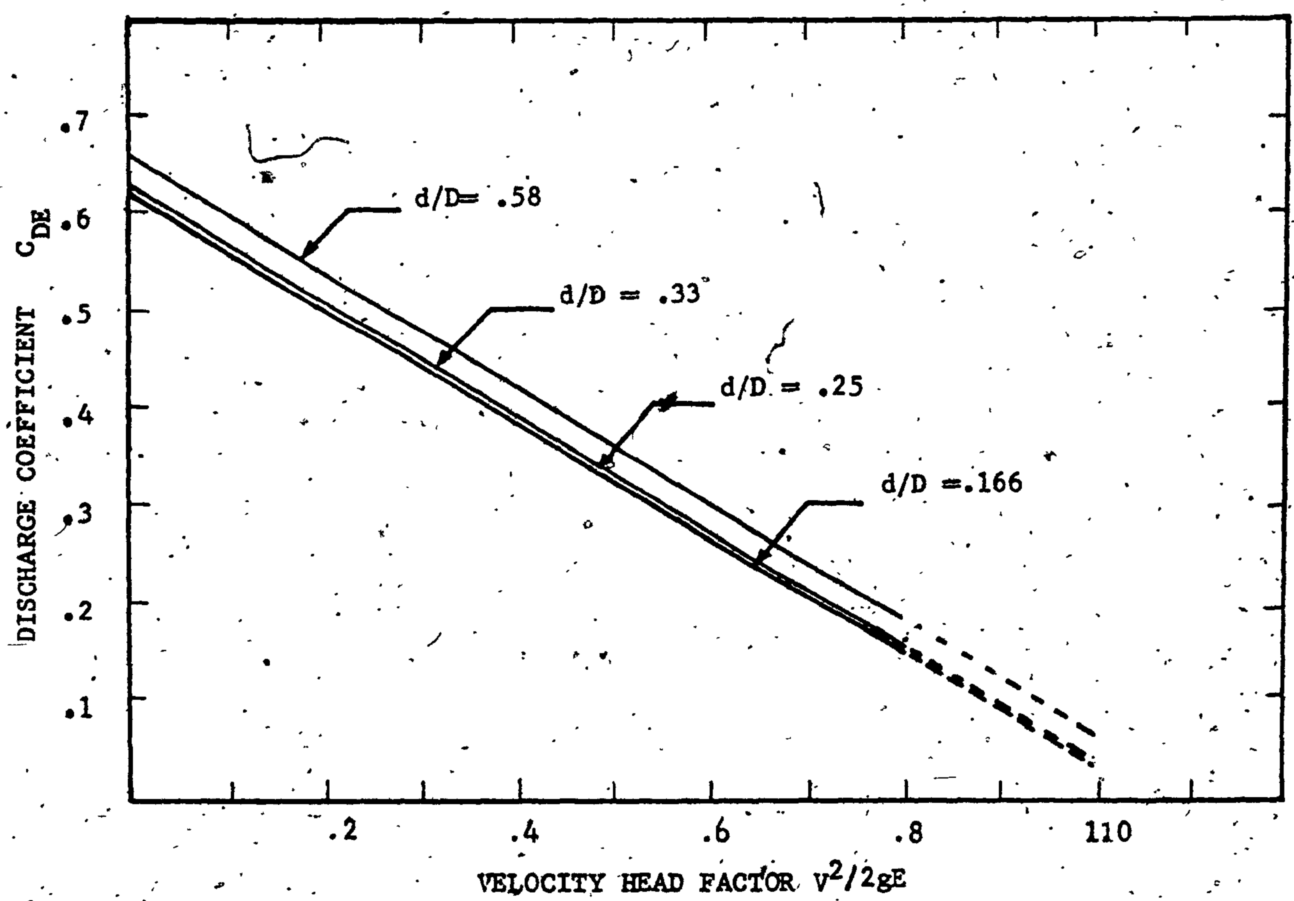

Fig. 8 - DISCHARGE COEFFICIENT FOR TESTED PIPES

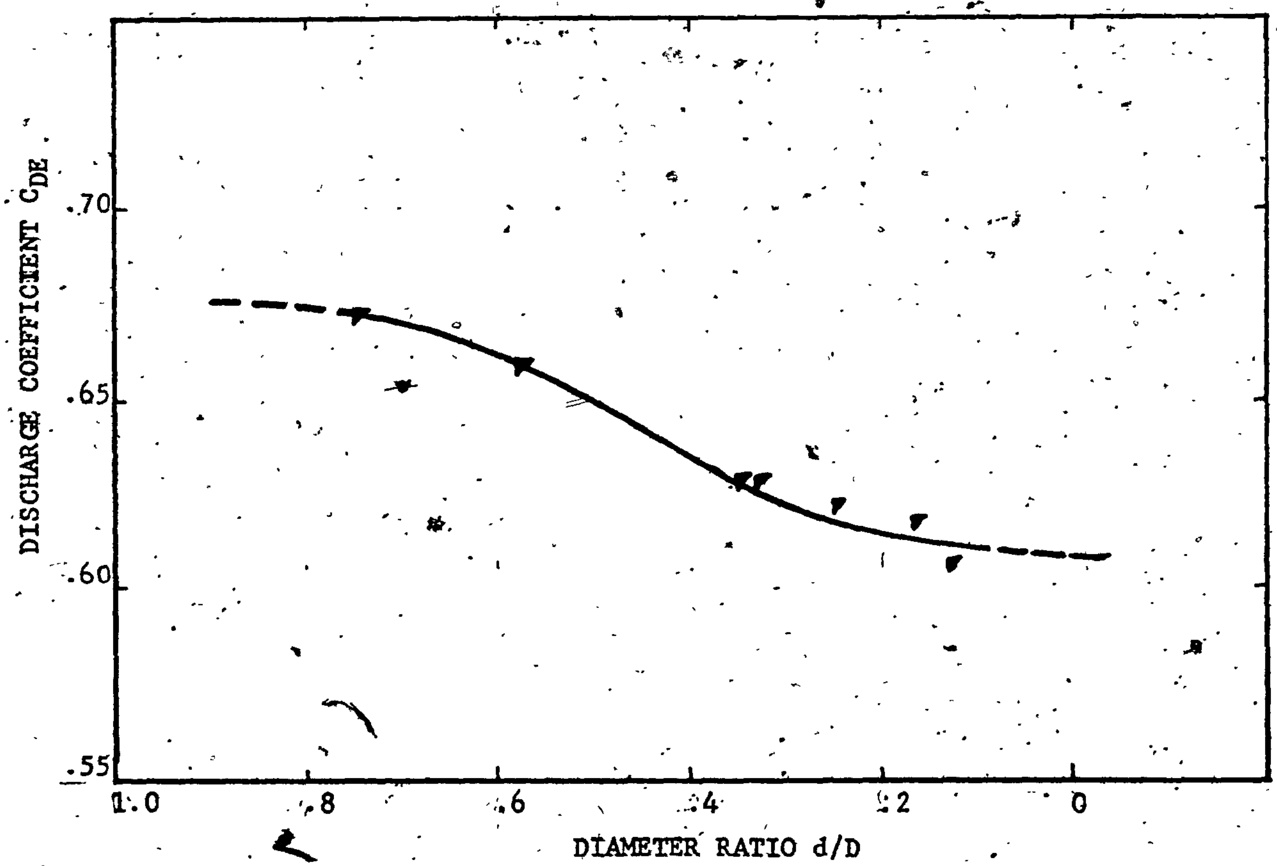

Fig. 9 - DISCHARGE COEFFICIENT FOR DEAD END PIPES

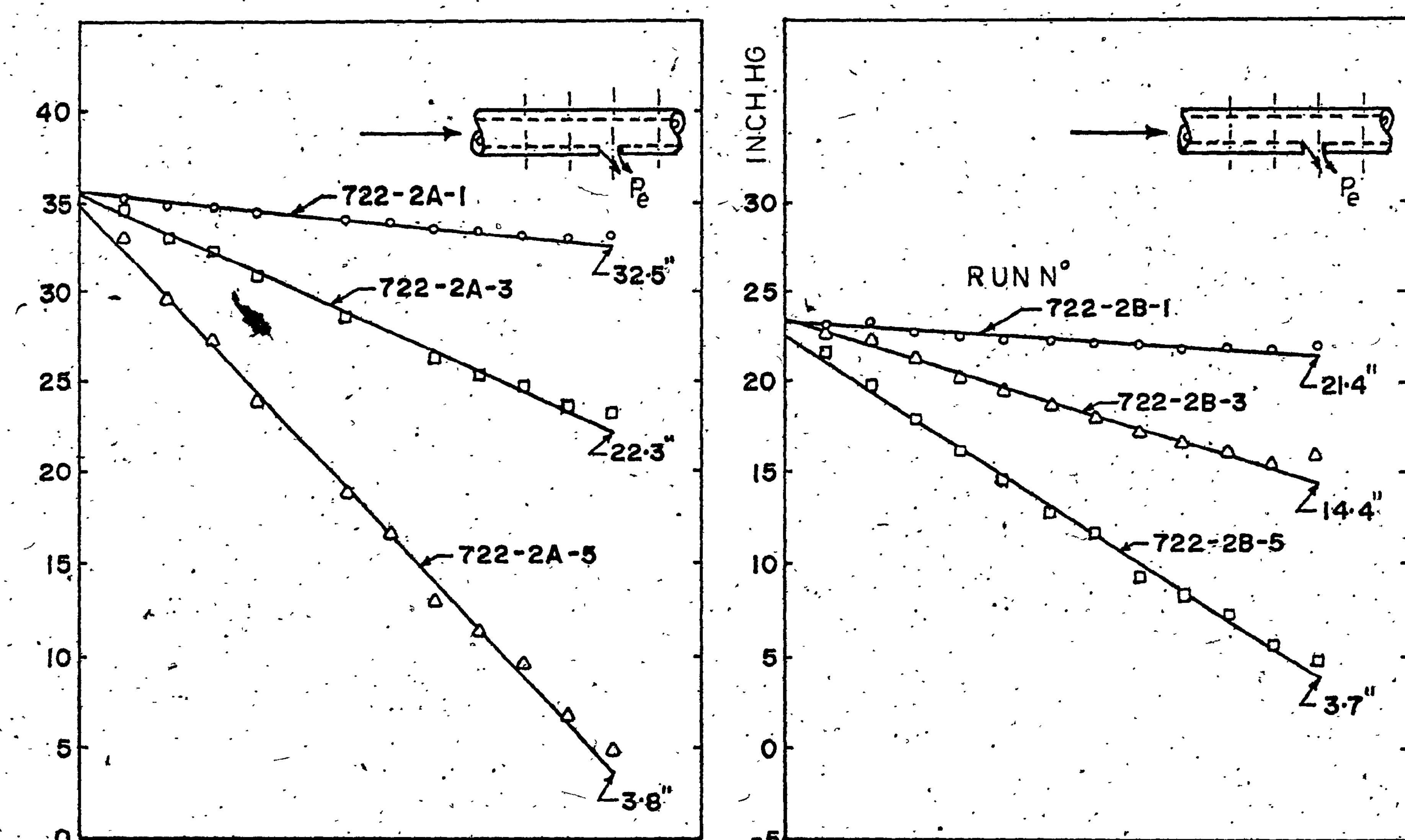

FIG.10a.PRESSURE GRADIENTS FOR PIPE NO. 1

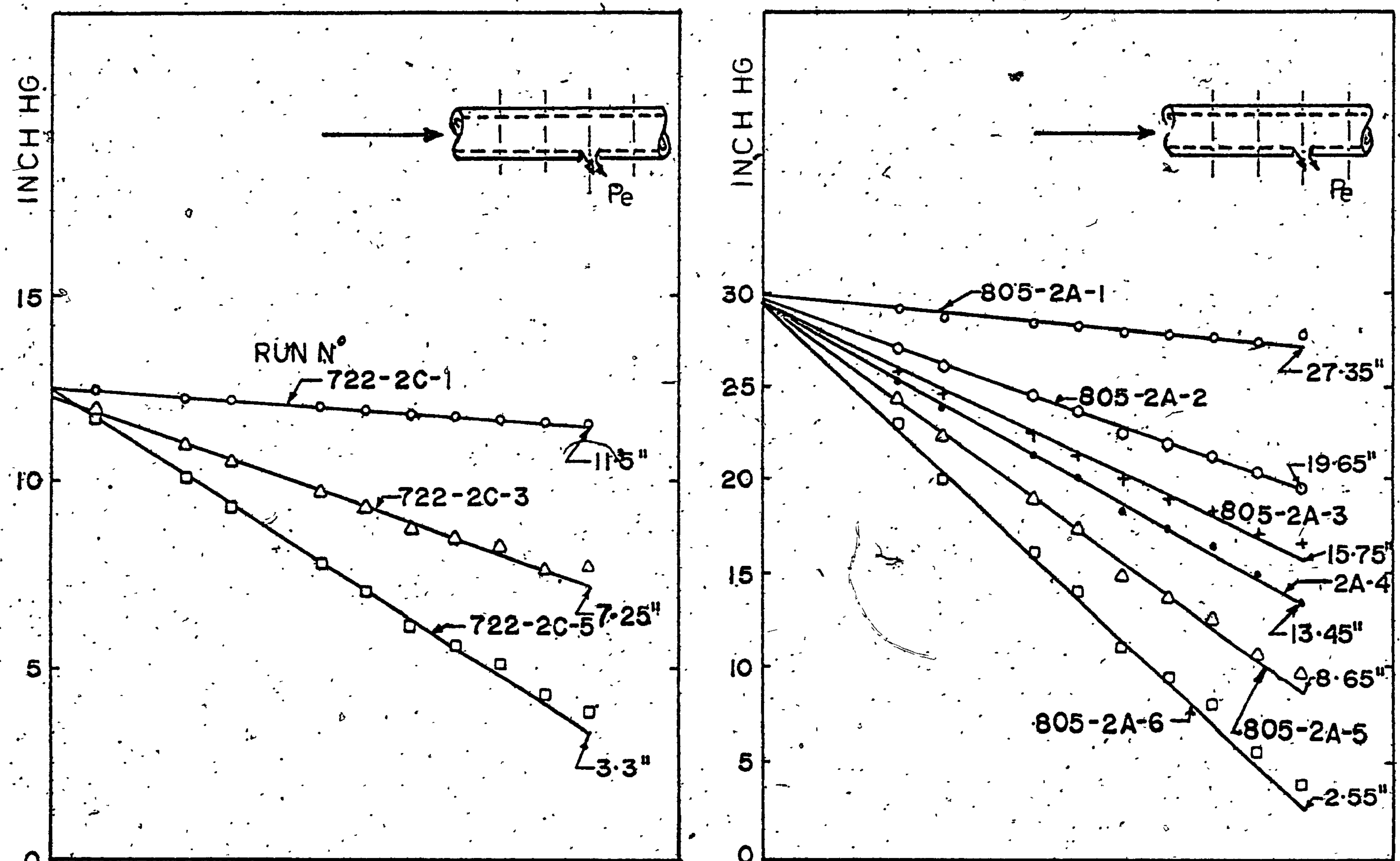

FIG.10b. PRESSURE GRADIENTS FOR PIPE NO. 1

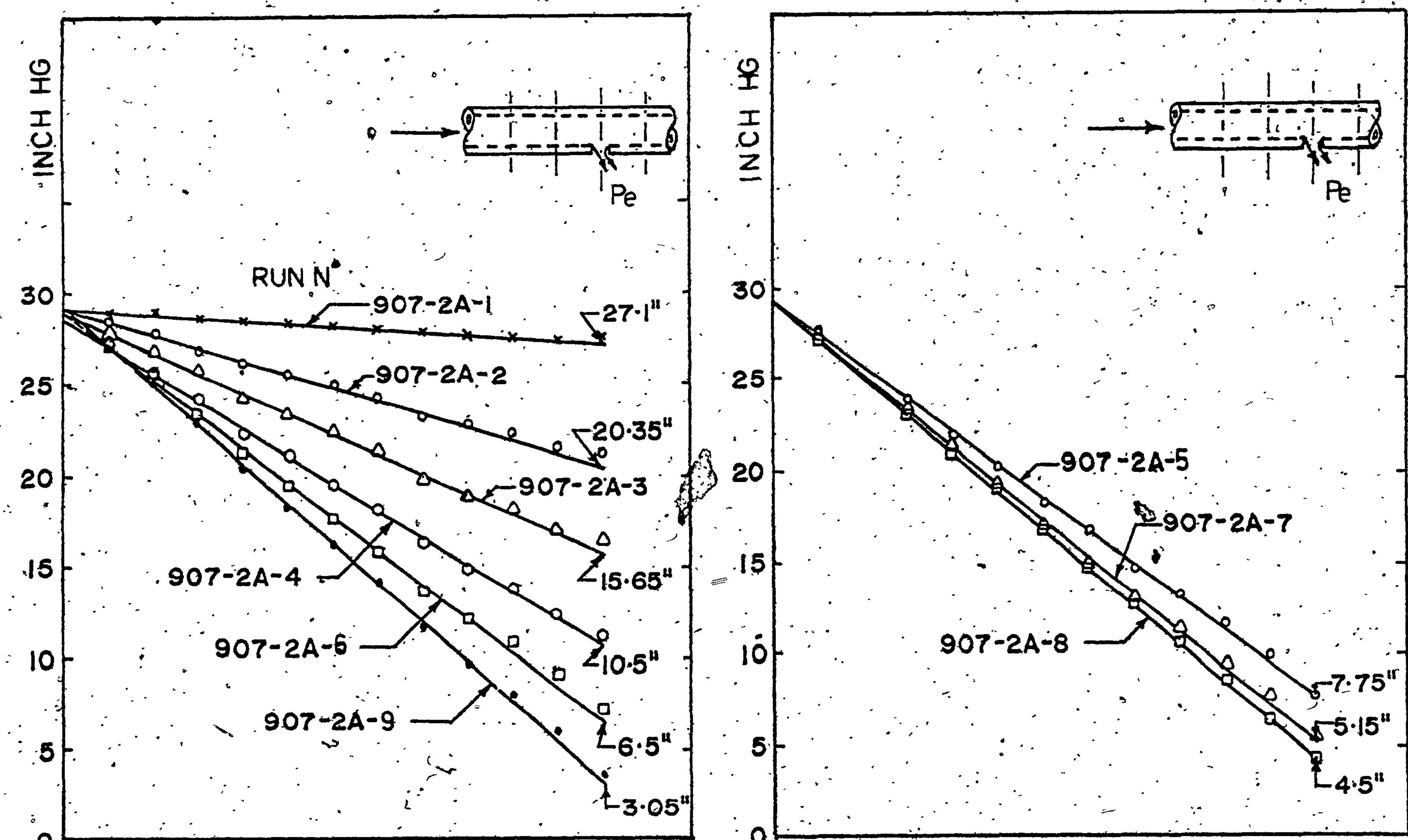

FIG.10c. PRESSURE GRADIENTS FOR PIPE NO. 1

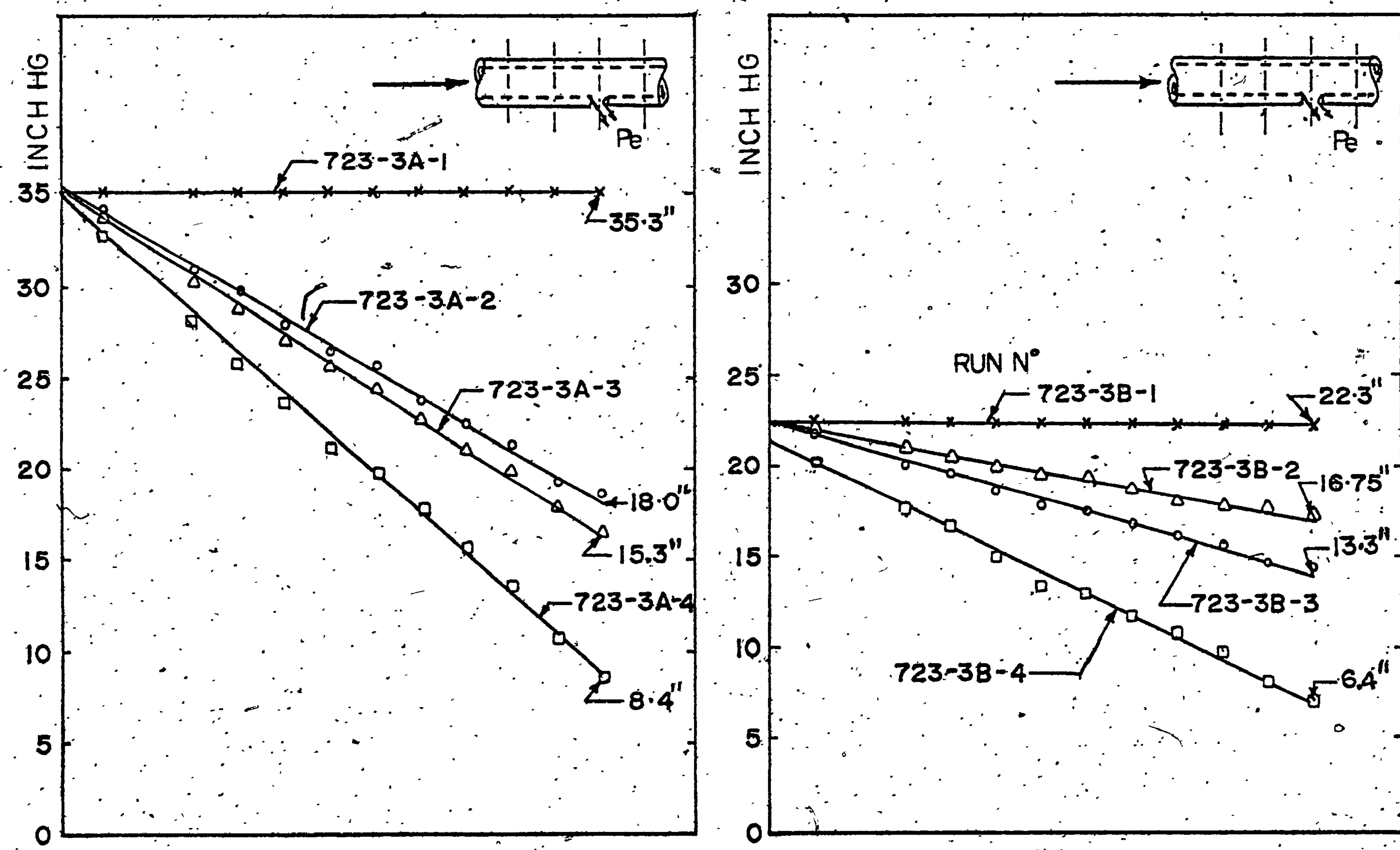

FIG. 11a. PRESSURE GRADIENTS FOR PIPE NO. 2

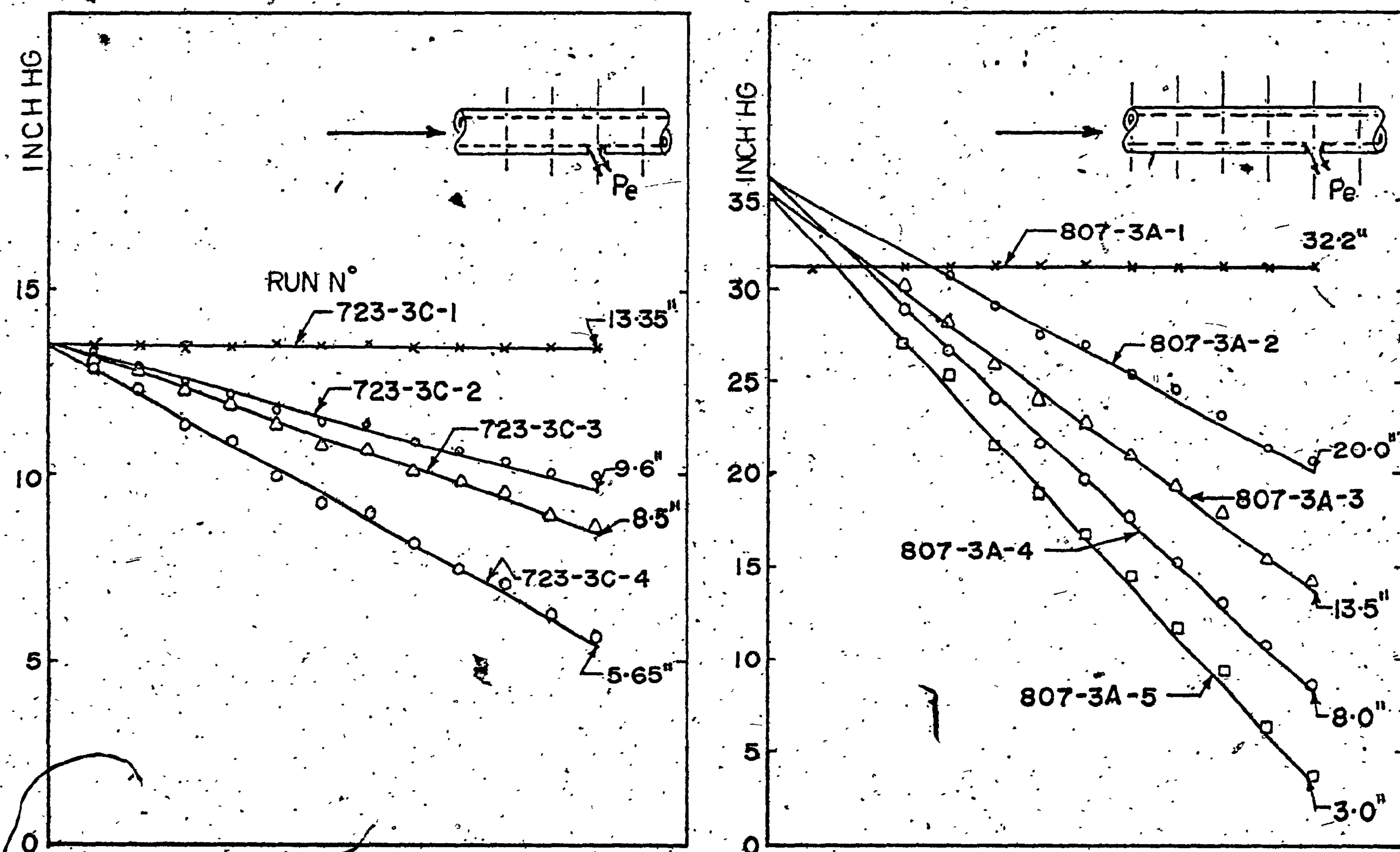

FIG. 11 b. PRESSURE GRADIENTS FOR PIPE NO. 2

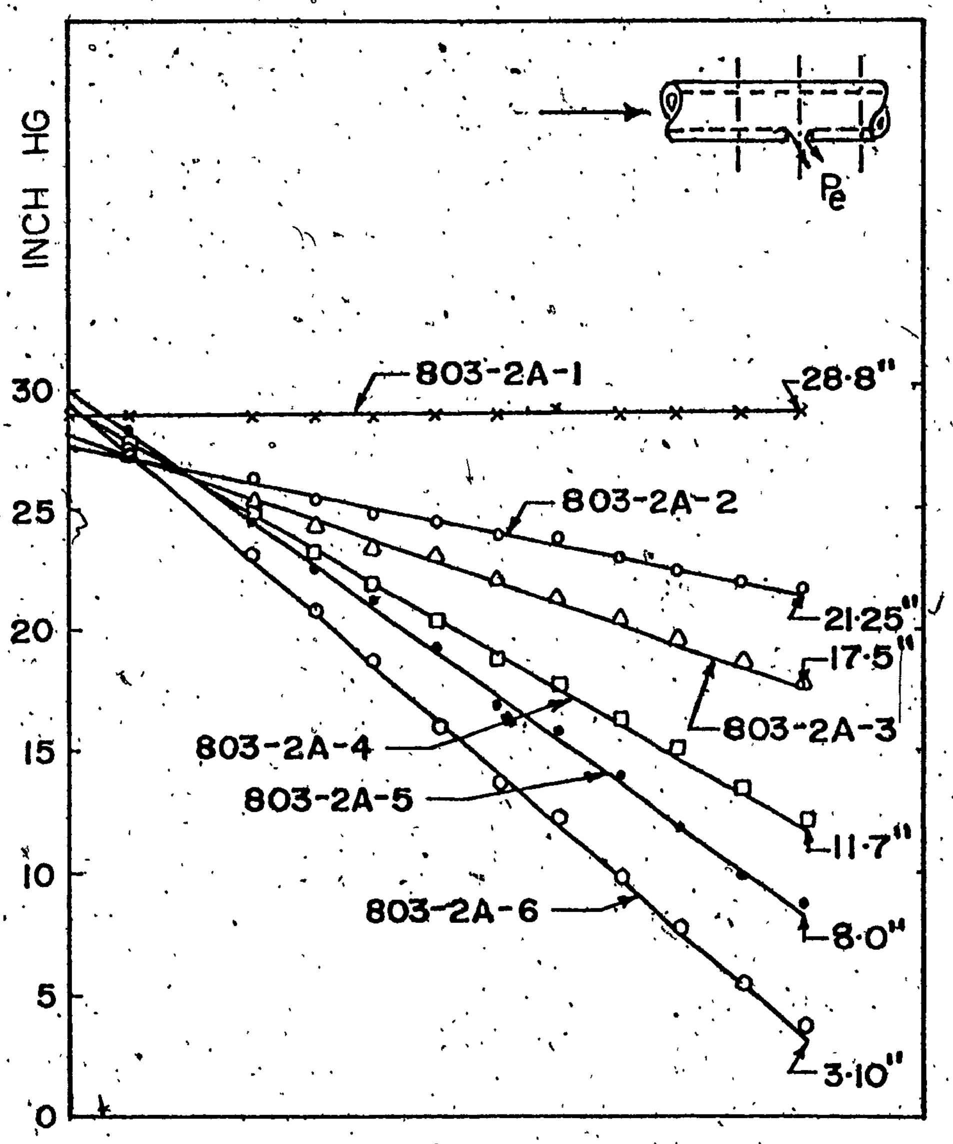

FIG. 12. PRESSURE GRADIENTS FOR PIPE NO. 3

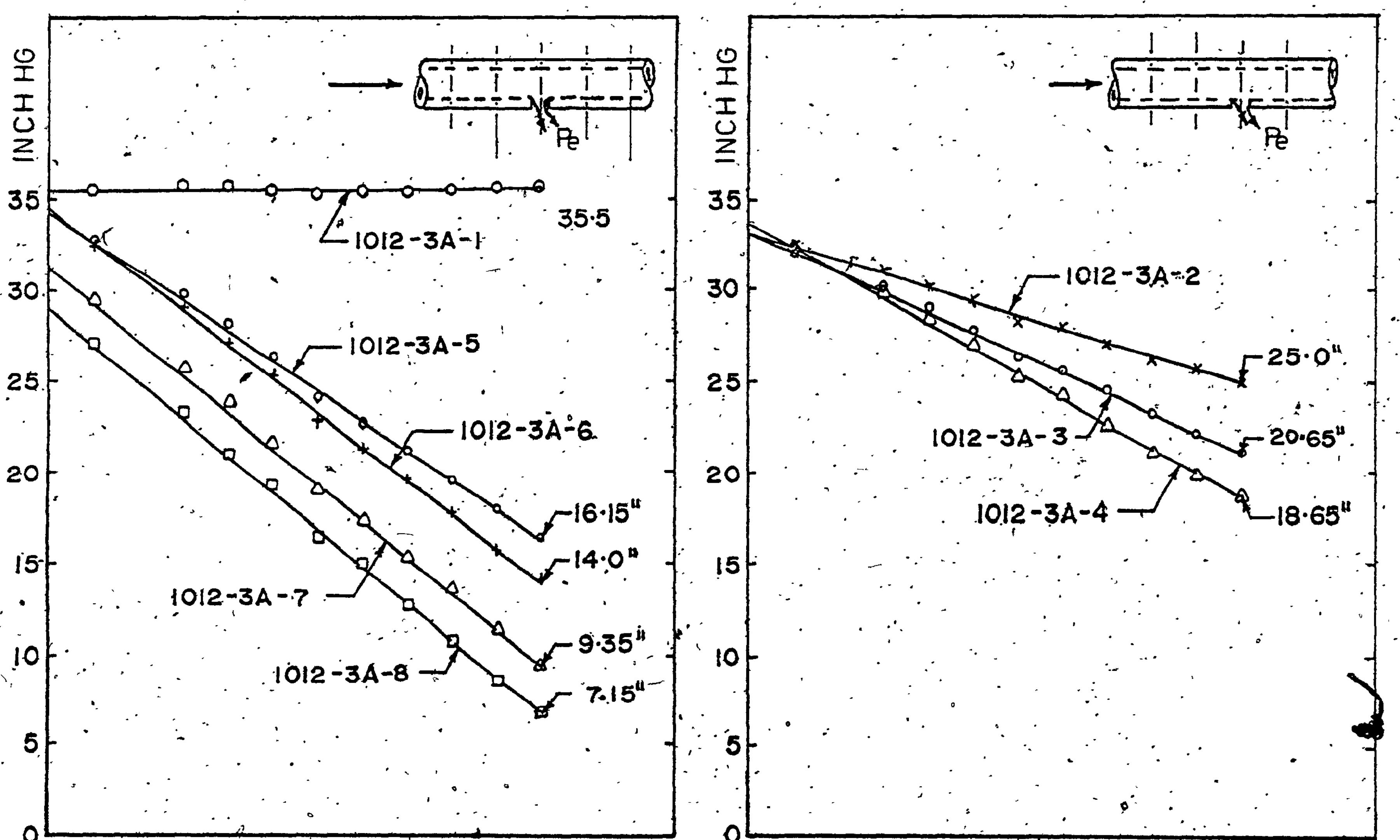

FIG. 13. PRESSURE GRADIENTS FOR PIPE NO. 4

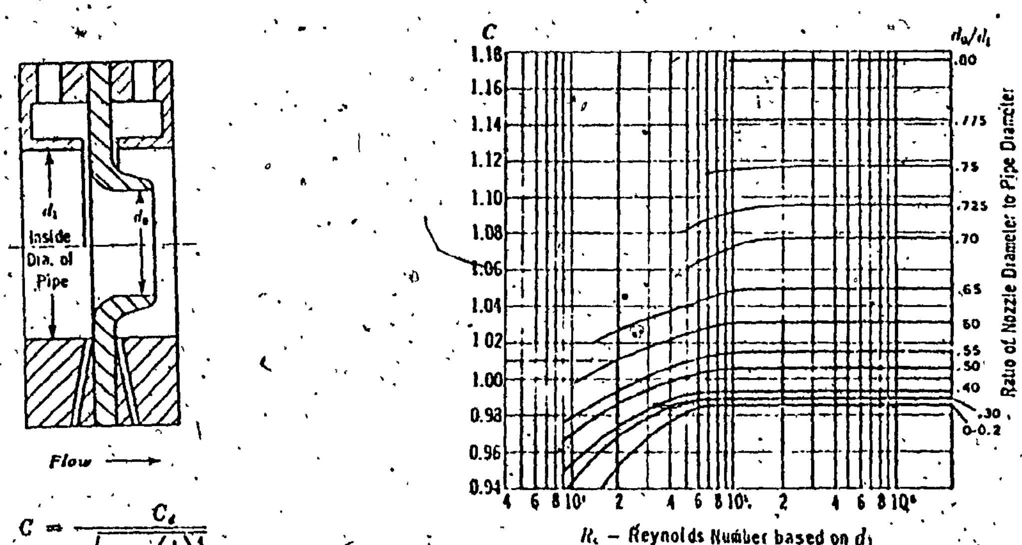

$$C = \frac{C_d}{\sqrt{1 - \left(\frac{d_0}{d_1}\right)^4}}$$

Fig. 14 - FLOW COEFFICIENT C FOR NOZZLES (9)

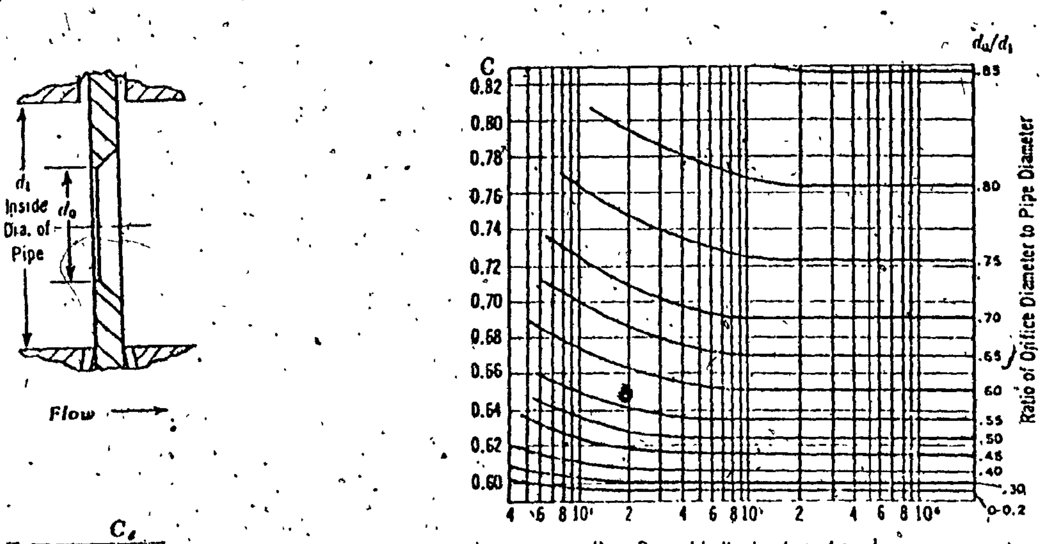

$$C = \frac{C_d}{\sqrt{1 - \left(\frac{d_0}{d_1}\right)^4}}$$

Fig. 15 - FLOW COEFFICIENT C FOR SQUARE EDGED ORIFICES (9)